Journal of the Korea Concrete Institute
Vol.17 No.4, pp.655~662, August, 2005

Effect of Moisture Loss on Development of Distresses in Concrete Pavements

Jin-Hoon Jeong[1)*]
[1)] Highway & Transportation Technology Institute, Korea Highway Corporation, 445-812, Korea

(Received December 10, 2004, Accepted July 30, 2005)

Abstract

Evaporation of concrete influences the development of both initial transverse cracking and delamination in the concrete slab. It was suggested that spalling distress might develop in the slab where the initial transverse cracking occurred by theoretical equations and a field investigation. Thus, efforts to prevent the evaporation of concrete using proper curing methods are required to minimize the distresses of the slabs. Effective curing thickness (ECT) concept was used in this paper to evaluate various curing methods used to prevent the evaporation from concrete. Curing effectiveness quantified by the ECT of different types and amounts of curing compound under various curing conditions was investigated based on the results of laboratory tests. According to the test results, the wind speed is inferred to be a significant factor of the magnitude and continuance duration of the curing effectiveness.

Keywords : ***concrete pavement, evaporation, curing, cracking, delamination, spalling***

1. Introduction

Water inside hardening concrete is categorized by two types. One is evaporable water existing in vapor of gel pores and capillary pores including intermediate layer, and the other is non-evaporable water structurally combining with hydration products[1)]. Because movement of water related to evaporation occurs mainly at the surface of concrete, larger moisture variation through depth of concrete pavement is observed near the top surface of the slab as shown in Fig. 1. The moisture distribution near the slab surface causes the deflection of slab such as warping at its early-age and delamination in the bonded overlay concrete pavement[2)].

Uncontrolled transverse cracking and delamination may develop at the top surface of the concrete slab due to restrained tensile strain caused by drying shrinkage. Prevention of the evaporation using proper curing methods can minimize the uncontrolled cracking and deformation of the early-age concrete slab. Generally curing compounds are used in the construction of concrete pavement to prevent the distresses. The curing effectiveness of the several types of curing compounds to prevent the distresses is evaluated in this paper by using the effective curing thickness (ECT) concept[3)].

2. Effect of evaporation on initial transverse cracking

Initial transverse cracking of concrete slab occurs at the point when tensile stress exceeds tensile strength at the slab top surface. Tensile stress of hardening concrete slab can be determined based on the following model using curling and warping behavior caused by the distribution of temperature and humidity within the slab[4,5)].

$$f_t = \frac{CE\varepsilon_t}{2(1-\nu)} \tag{1}$$

where

f_t = tensile stress of slab

C = stress coefficient of slab

$$= 1 - \frac{2\cos\lambda\cosh\lambda(\tan\lambda - \tanh\lambda)}{\sin 2\lambda \sinh 2\lambda}$$

* Corresponding author
E-mail address: j-jeong@freeway.co.kr

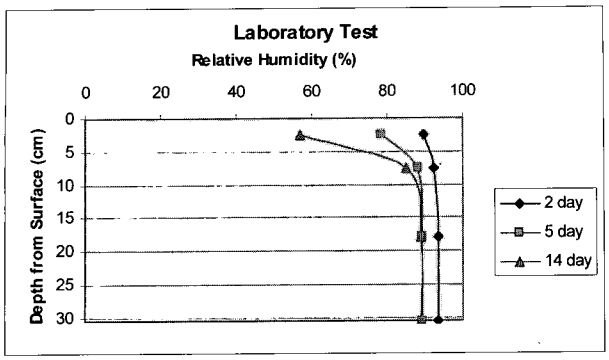

(a) Moisture profiles of a specimen cured in laboratory

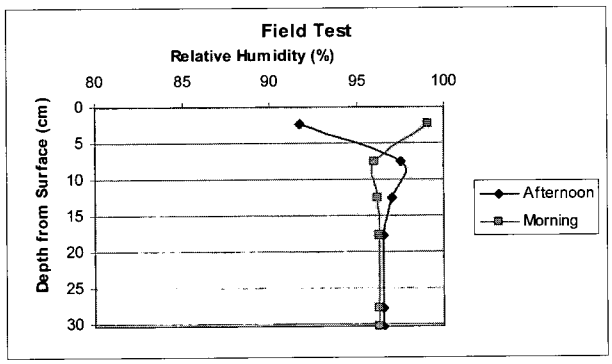

(b) Moisture profiles of a test slab cured in field

Fig. 1 Moisture variation through depth of concrete pavement

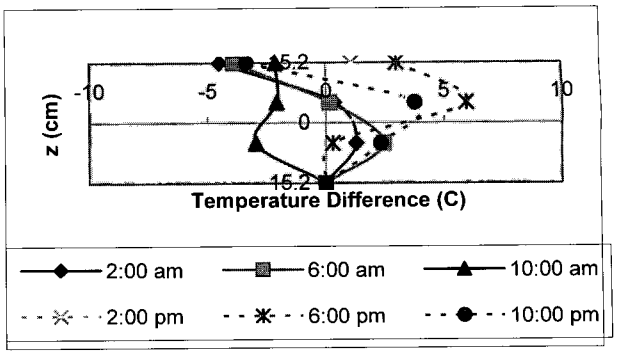

(a) Temperature difference

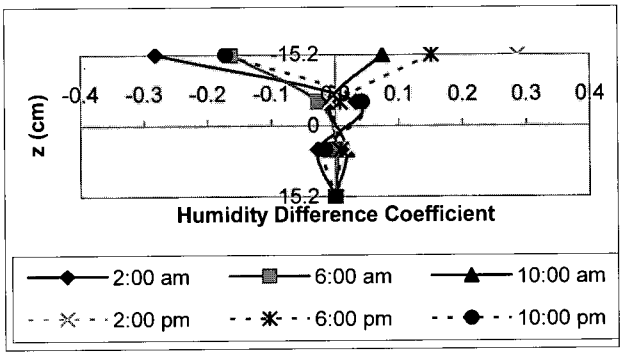

(b) Humidity difference coefficient

Fig. 2 Temperature difference and humidity difference coefficient between a depth and bottom of a test slab

$\lambda = \frac{L}{\ell\sqrt{8}}$

L = length or width of slab

ℓ = radius of relative stiffness

E = elastic modulus of concrete

ν = Poisson's ration of concrete

ε_t = strain due to curling and warping
$= \alpha_t \Delta T_{eq} - \varepsilon_{sh\infty} \Delta (1 - H^3)_{eq}$

α_t = coefficient of thermal expansion (CoTE)

$\varepsilon_{sh\infty}$ = ultimate drying shrinkage

Temperature distribution from top to bottom of slab is nonlinear like humidity distribution shown in Fig. 1. Thus, the profile of temperature and moisture differences through slab depth is nonlinear. The profiles of temperature and moisture differences need to be expressed by third polynomial functions to determine effective linear differences of temperature or humidity between top and bottom of the slab[6]. The temperature difference between top and bottom of the slab (Fig. 2 (a)) is expressed by third polynomial function as:

$$\Delta T(z) = A + Bz + Cz^2 + Dz^3 \quad (2)$$

In the coordinate system (z) of the function, upward from the mid-depth of the slab is negative and downward is positive. The equivalent linear temperature difference between top and bottom of the slab which causes same slab curvature as that due to above nonlinear temperature distribution is calculated by following procedure. The equivalent linear temperature difference is used in equation (1) to calculate strain of slab top surface.

$$\Delta T_{eq} = -\frac{12M^*}{\alpha_t h^2}$$

where

$$M^* = \int_{-\frac{h}{2}}^{\frac{h}{2}} \alpha_t \Delta T(z) z dz$$

$$= \alpha_t \left(B\frac{h^3}{12} + D\frac{h^5}{80} \right)$$

h = slab thickness

therefore

$$\Delta T_{eq} = -12\left(\frac{Bh}{12} + \frac{Dh^3}{80} \right) \quad (3)$$

Humidity effect mainly caused by evaporation can also be considered following the same procedure as the calculation of equivalent linear temperature difference. Humidity difference coefficient, $\Delta(1\text{-}H^3)_{eq}$, at each depth was devel-

oped based on drying shrinkage model suggested by Bazant and Najjar as[7]:

$$\varepsilon_{sh} = \varepsilon_{sh\infty}\left(1 - H^3\right)$$

where H is humidity of concrete specimen. Because the humidity difference coefficient is also nonlinear through slab depth as shown in Fig. 2 (b), equivalent linear humidity difference coefficient, $\Delta(1\text{-}H^3)_{eq}$, is calculated by following equation (2) and (3)[5]. The equivalent linear humidity difference coefficient has the same role as the equivalent linear temperature difference in the calculation of slab behavior.

3. Effect of evaporation on delamination

Delamination is also influenced by humidity distribution through the slab depth at its early-age. Warping behavior due to the humidity distribution causes relatively large shear stress in the slab. Because of the shear stress, delamination can develop at corner or joint of the slab[2]. The delamination is mostly found near top surface of the slab where moisture variation through depth is relatively large, and sometimes develops into large scale of spalling. Occasionally, because of the concentration of stress to weak points, horizontal cracking is observed at the position of rebar and dowel bar. The horizontal cracking at the positions is also due to humidity variation caused by evaporation. The shear stress which causes delamination is calculated by following procedure using curling and warping behavior of the slab based on the mid-thickness plate theory. To calculate the deflection of corner or edge of the slab, the similar type of following equation to that suggested by Tang et al. is used[8].

$$w = \frac{(A_1\cos x + A_2\sin x)(B_1\cos y\cosh y + B_2\sin y\sinh y)}{e^{\sigma}} \quad (4)$$

The shear or delamination stress (τ_{xy}) is derived from plate theory using the curling and warping curvature (equation (5)) calculated by differentiating the equation (4) as:

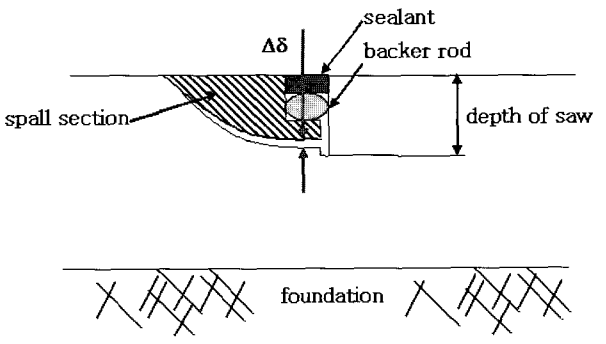

Fig. 3 Opening of delamination in jointed concrete pavement that causes spalling distress

$$\tau_{xy} = \frac{Ez}{1+\nu} w_{,xy} \quad (5)$$

where

z = distance from mid-depth of slab

$$w_{,xy} = \frac{\left[\cos x(A_2 - A_1) - \sin x(A_2 + A_1)\right]\left[(B_2 - B_1)\sin y\cosh y + (B_2 + B_1)\cos y\sinh y\right]}{e^{\sigma}\ell^2}$$

$$x = \frac{X}{\ell}$$

$$y = \frac{Y}{\ell}$$

X = distance from slab corner in longitudinal direction

Y = distance from slab corner in transverse direction

Coefficient equations, A_1, A_2, B_1, and B_2, shown in equation (4) and (5) are calculated by categorizing the curing and warping behavior as liftoff case and zero-liftoff case as:

Liftoff case

$$A_1 = T_R A_2 \quad (6)$$

$$A_2 = \frac{w_0 e^{-\sigma}\left(1 - \frac{s^3}{3\lambda^2}\right)}{\nu B_2\sin s' + B_1\cos s' - T_R\left(B_1\sin s' + \nu B_2\cos s'\right)}$$

$$B_1 = 1$$

$$B_2 = \frac{w_0 s^2}{2\lambda A_2\left(T_R - 1\right)}\left[1 + \frac{(T_R C_2 - C_1)(T_R + 1)}{(T_R C_1 - C_2)(T_R - 1)}\right]^{-1}$$

Zero-liftoff case

$$A_1 = T_R A_2$$

$$A_2 = \frac{w_0}{B_1 - \nu B_2 T_R}$$

$$B_1 = 1$$

$$B_2 = B_1\frac{T_R - 1}{T_R + 1}$$

where

$$T_R = \frac{1 - \tan\frac{W}{2\lambda}}{1 + \tan\frac{W}{2\lambda}}$$

$$w_0 = A_0\left(1 + \nu\right)\lambda^2$$

$$A_0 = \frac{\varepsilon_t}{h}$$

$$C_1 = \cos s' - \sin s'$$

$$C_2 = \cos s' + \sin s'$$

$$s' = \frac{s}{\lambda}$$

Table 1 shows the key parameters and its symbols included in the coefficient equations of curling and warping. The curling and warping strain (ε_t) shown in equation (6) is the

Table 1 Key parameters used in curling and warping coefficient equations

Parameters	Symbols
Ultimate drying shrinkage of concrete	$\varepsilon_{sh\infty}$
Concrete humidity	H
Concrete CoTE	α_t
Concrete temperature	T
Slab thickness	h
Slab width	W
Concrete Poison's Ratio	ν
Radius of relative stiffness	ℓ
Length of liftoff	s
Edge gap	w_0

same strain used in equation (1) to calculate the initial transverse cracking.

4. Development of spalling

The pre-existing delamination to the pavement surface due to tensile stress induced mainly by wheel loading (Fig. 3). It is first necessary to determine the opening of the delamination ($\Delta\delta$) to calculate the tensile stress. To calculate the delamination opening, joint stiffness needs to be known as:

$$J = \frac{D}{s_d k\ell} + \frac{agg}{k\ell}$$

where

J = joint stiffness
D = dowel contribution to joint stiffness
agg = aggregate interlock contribution to joint stiffness
s_d = dowel spacing
k = modulus of soil reaction

The load transfer efficiency (LTE) model is used to calculate the joint stiffness based on the width of the crack or joint. The delamination opening is also related to the difference between the unloaded and loaded slab deflection along the joint or crack. The dimensionless unloaded edge deflection (δ_u^*) can be calculated as[9]:

$$\delta_u^* = 0.215\left[\frac{J - 0.6\log(1+J)}{J+0.4}\right]\left\{1 - 0.7\frac{a_L}{\ell}\left[1 + 0.06\log(1+J) - 0.01J^{0.2}\right]\right\}$$

where a_L is radius of tire contact area. The unloaded edge deflection (δ_u) can be calculated as a function of load, modulus of soil reaction, and radius of relative stiffness as:

$$\delta_u = \frac{\delta_u^* P_i}{k\ell^2} \tag{7}$$

where P_i is traffic load on pavement. The dimensionless loaded edge deflection (δ_f^*) can be calculated in a similar fashion as the dimensionless unloaded edge deflection as[9]:

$$\delta_f^* = 0.4314 - 0.351\left(\frac{a_L}{\ell}\right) + \frac{0.1468}{2}\left(\frac{a_L}{\ell}\right)^2$$

The loaded edge deflection is calculated using:

$$\delta_f = \frac{\delta_f^* P_i}{k\ell^2} \tag{8}$$

By subtracting equation (7) from equation (8), the deflection difference between the loaded and unloaded slabs is obtained.

$$\delta_l = \delta_f - \delta_u$$

The opening of the delamination is related to LTE_δ as:

$$\Delta\delta = \delta_l\left(1 - \frac{LTE_\delta}{100}\right)$$

The bending load on the piece of spalled concrete is related to the shear resistance acting along the interface of the joint or crack. The influence of aggregate interlock on the shear resistance along this interface is calculated as:

$$T_{agg} = \frac{0.0312h^{1.4578}e^{-0.039cw}P_i}{h^2}$$

where

T_{agg} = aggregate interlock shear stress
cw = crack width (mills)

In addition, the shear stress contribution of the joint seal material acting on the spalled concrete is calculated as:

$$T_s = G_{seal}\gamma_{seal}$$

where

T_s = joint seal shear stress
G_{seal} = shear modulus of joint sealant
$= \dfrac{E_{seal}}{2(1+\nu_{seal})}$
E_{seal} = stiffness of joint sealant
ν_{seal} = Poisson's ration of joint sealant
γ_{seal} = ratio of delamination opening to the joint seal width

$$= \frac{\Delta\delta}{W}$$

W = joint seal width

By averaging the shear stresses due to aggregate and joint sealant over the distance where those act, it is possible to calculate the shear resistance to spalling an the joint.

$$s = T_s \frac{d_s}{2} + T_{agg}\left[t - d_{sawcut}\left(1 - \frac{n_1 \Delta t}{100}\right)\right]\left(\frac{LTE_\delta}{100}\right)$$

where

s = shear resistance to spalling at the joint

d_s = depth of seal

t = depth of spall

d_{sawcut} = depth of saw-cut

n_1 = % joints per time filled with incompressibles

Δt = time since joints were cleaned and sealed

If $d_{sawcut}\left(1 - \frac{n_1 \Delta t}{100}\right)$ is larger than depth of spall, then aggregate interlock shear resistance equals zero since there is not aggregate contact within the depth of the spall. Based on a weighting between the shear due to the joint sealant and the shear on the crack face, the bending moment per unit width is calculated as:

$$M = sl^*$$

where

M = bending load to cause spall

l^* = length of delamination (based on the % of spalling)

To determine if a spall will form, it is necessary to predict the magnitude of the tensile stress (σ_{spall}) acting on the spalled section. First, the frictional shear stress (τ_f) at the bottom of the delamination is determined as:

$$\tau_f = \frac{0.25e^{-0.039\Delta\delta} P_i}{h^2}$$

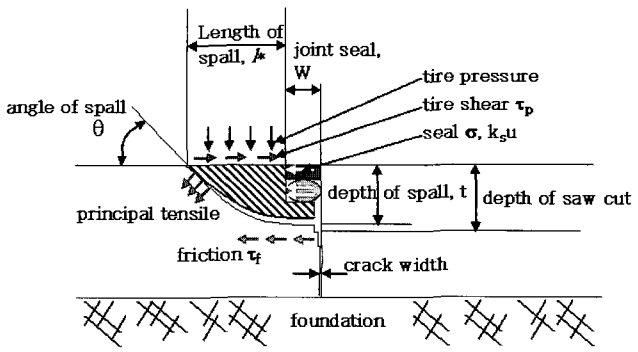

Fig. 4 Concrete pavement spalling schematic

The frictional resistance is then input to equation (9) for the calculation of the tensile stresses that cause spalling.[2] The parameters shown in the equation is depicted in Fig. 4.

$$\sigma_{spall} = \frac{1}{\sin\theta}\left[(\tau_p - \tau_f)\frac{l^*}{t} + \frac{\tau_f}{\tan\theta} + \frac{k_s u}{t}\right] + \frac{6M}{t^2} \quad (9)$$

where

τ_p = shear stress from tire loading (> 25 psi)

θ = angle of spall fracture (assumed to be 60°)

k_s = stiffness of joint sealant

$= \frac{E_{seal}}{d_s}$

u = thermal displacement at joint

$= \alpha_t \Delta T L$

5. Relation between initial transverse cracking and spalling

Initial transverse cracking and delamination may occur at the same time in early-age concrete slab because of large change in humidity through depth due to evaporation at the slab top surface. A specimen cored from a jointed plain concrete pavement (JPCP) slab with transverse cracking due to initial evaporation is compared to a specimen cored from another JPCP slab under good condition due to a proper curing application as shown in Fig. 5. Delamination was observed between approximately 25 mm (1 inch) and

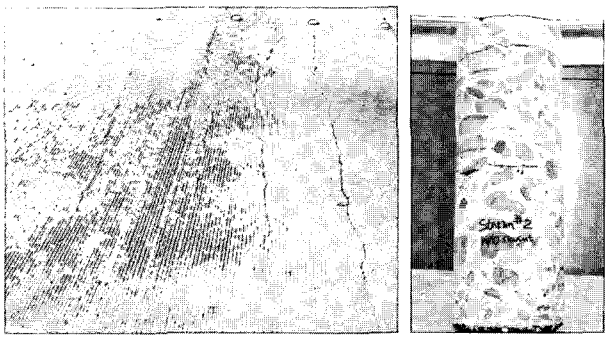

(a) A core of a slab with densely spaced initial transverse cracking

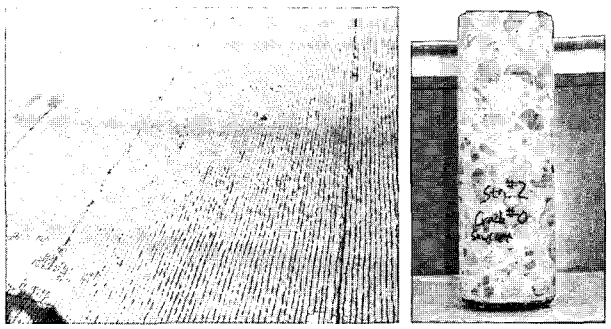

(b) A core of a slab without any cracking

Fig. 5 Delamination cracking observed at a slab with initial transverse cracking

51 mm (2 inch) from top surface of the specimen cored from the transversely cracked slab while delamination was not observed at the specimen cored from the slab under good condition. The delamination occurred during paving or immediately after paving can develop into spalling distress because of repetitive wheel loads, freezing and thawing, and imcompressibles intruded into cracks or joints. Therefore, it is expected that the slab with initial transverse cracking will experience more spalling distress than the slab used proper curing method to prevent the cracking as shown in Fig. 6.

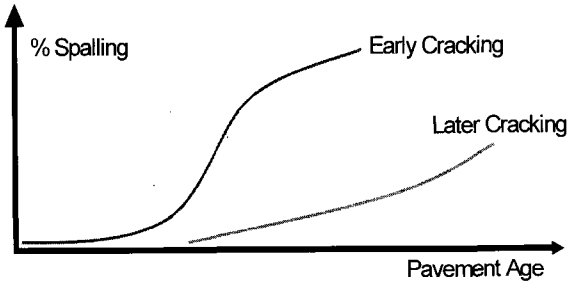

Fig. 6 Expected relation between development of initial transverse cracking and spalling distress

6. Quantification of curing effectiveness

Relatively large variation of humidity through depth is observed near top surface of the slab because moisture evaporates at the slab surface with hardening of concrete. If the evaporation can be minimized by proper curing methods, the humidity would be almost constant from top to bottom of the slab by the effect of membrane formed on the slab surface. Based on the concept, the effectiveness of curing was formularized by Bazant and Najjar using the humidity at ambient, concrete surface, and inside concrete as the parameters as[10].

$$L = \frac{\ln\left(\frac{H_s}{H_a}\right)}{\frac{\partial H_s}{\partial x}}$$

where

L = ECT

H_s = humidity at concrete surface

H_a = ambient humidity

The ECT can be defined as the imaginary additional thickness of the slab to express the level of curing. The surface humidity of the slab under poor curing condition should be lower than that under better curing condition. Thus, the humidity of the slab under worse curing condition becomes same at its certain depth as the surface humidity of the slab under better curing condition. Therefore, considering the humidity, it can be postulated that the slab under better curing condition has more imaginary thickness than the other slab. The humidity at ambient, concrete surface, and 19 mm (0.75 inch) depth of concrete needs to be measured as shown in Fig. 7 to quantify the curing effectiveness using the above concept[3].

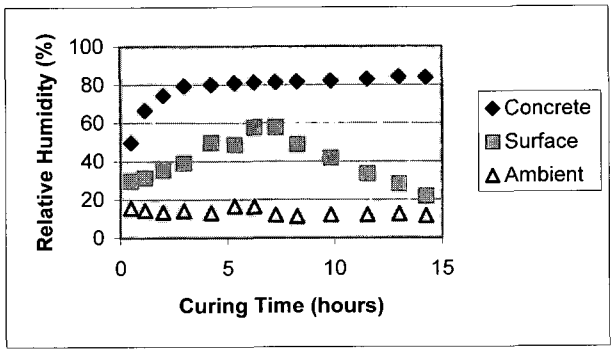

Fig. 7 Changes in concrete relative humidity with curing time at different positions (zero wind speed)

7. Evaluation of curing compounds

The most common curing method for the concrete pavement is spraying curing compound on its whole surface immediately after placing the concrete. Preliminary test results for the effects of different types of curing compounds under different environmental conditions are presented in this paper. Wax-type, resin-type, and acrylic-type curing compounds dissolved in water or solvent are mainly used for curing of the concrete pavement. The properties of the wax-type and resin-type curing compounds used in this study are shown in Table 2.

Fig. 8 shows the decrease of amount of evaporation and rate of evaporation by applying the resin-type curing compound on the top surface of concrete specimen placed in 300 mm (12 inch) diameter and 150 mm (6 inch) height of PVC cylindrical ring. The concrete specimen was cured in a curing chamber with 32 °C temperature, 50 % relative humidity, and 5.33 m/s wind speed. The mixture proportions of the concrete are shown in Table 3. Effect of amount of curing compound was also investigated by applying different amount of wax-type curing compound on the concrete specimen under the same curing temperature and relative humidity at zero wind speed. The ECT of the concrete was compared for three cases: no application, one-time application(5.0 m^2/liter/time[11]), and three-times application. The ECT substantially increased as the amount of curing compound

Table 2 Properties of curing compounds used in this study

Types	Volatile organic content (g/l)	Drying time (hours at 21 °C)
Wax	0	1
Resin	74	2

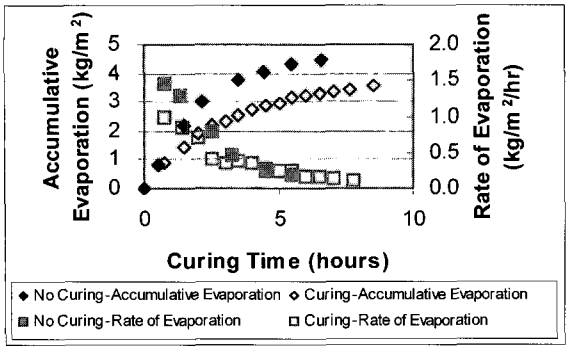

Fig. 8 Decrease of evaporation by using curing compound (5.33 m/s of wind speed)

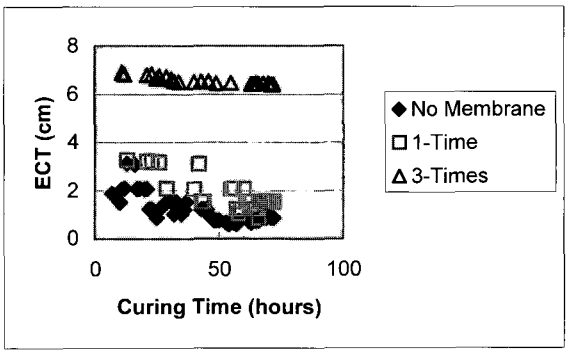

Fig. 9 Changes in ECT with different amount of curing compound (zero wind speed)

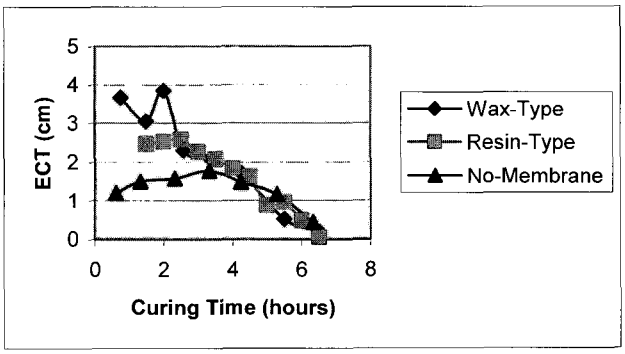

(a) 2.08 m/s of wind speed

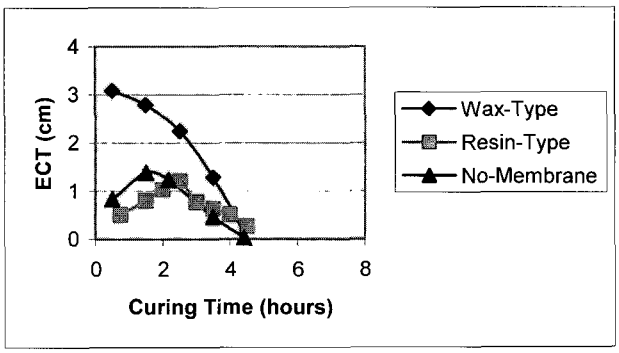

(b) 5.33 m/s of wind speed

Fig. 10 Changes in ECT with different types of curing compound and different wind speeds

increased (Fig. 9). The ECT steadily decreased with time for all cases because the effectiveness of the curing compounds dropped. Faster decrease rate of ECT was observed for the concrete which used less amount of curing compound on it.

The effects of wax-type and resin-type curing compounds were investigated at different wind speeds of 2.08 m/s and 5.33 m/s in a laboratory with 40 °C and 15 % of temperature and relative humidity. The concrete cured by the curing compounds had larger value of ECT than the concrete without any curing compound applications as shown in Fig. 10. The effect of curing was also maintained for the concrete cured by the curing compounds for a longer time. The noteworthy point in this test is that the curing effectiveness decreased rapidly and substantially as the wind speed increased. Therefore, the distresses due to evaporation would be significantly reduced by enhancing the curing effectiveness if the influence of wind at the construction sites of concrete pavements can be properly controlled.

8. Conclusions

Substantial variation of humidity through depth is observed near top surface of the concrete slab due to evaporation at its early-age. The result of a field investigation implied that the initial transverse cracking may occur at the same time as the delamination because of the large amount of evaporation. Moisture effect on the development of delamination near the slab surface was larger than temperature effect. The delamination occurred under the severe curing conditions can develop into spalling in large scale with curing time. Controlling the evaporation using proper curing methods immediately after construction is important to minimize the cracking and spalling distresses. Effects of different types of curing compounds were investigated under various conditions using ECT concept. The concrete used larger amount of curing compound had higher curing effect, and the effect continued for a longer time. Wind

Table 3 Mixture proportions of 1 m^3 of concrete used in laboratory tests

Curing conditions	32 °C, 50 %	40 °C, 15 %
CA (limestone)	1,068 kg	1,143 kg
FA (natural sand)	704 kg	753 kg
Cement	337 kg	360 kg
Water	137 kg	166 kg
W/C ratio	0.41	0.46
Air entraint	0.2 liters	-
Water reducer	1.1 liters	-
Unit weight of conc.	2,247 kg/m^3	2,422 kg/m^3

speed significantly reduced the curing effect and shortened curing duration. Considering the fact that the curing effectiveness rapidly decreased as the wind speed increased, further active efforts to minimize the effect of wind in construction sites of concrete pavements are essential.

References

1. Mindess, S. and Young, J. F., *Concrete*, Prentice-Hall, Inc., Englewood Cliffs, NJ, 1981.
2. Wang, L. and Zollinger, D. G., "A Mechanistic Design Framework for Spalling Distress", *Transportation Research Record 1730,* TRB, National Research Council, Washington, DC, 2000, pp.18~24.
3. Jeong, J. H. and Zollinger, D. G. *Development of Test Methodology and Model for Evaluation of Curing Effectiveness in Concrete Pavement Construction*, Transportation Research Record 1861, TRB, National Research Council, Washington D.C., 2003, pp.18~25.
4. Huang, H. H., *Pavement Analysis and Design.* Prentice-Hall, Inc., Englewood Cliffs, NJ, 1993.
5. Jeong, J. H. and Zollinger, D. G., "Environmental Effects on the Behavior of Jointed Plain Concrete Pavements", *Journal of Transportation Engineering*, ASCE, Vol.131, No.2, 2005, pp.140~148.
6. Mohamed, A. R. and Hansen, W., *Effect of Nonlinear Temperature Gradient on Curling stress in Concrete Pavement*, Transportation Research Record 1568, TRB, National Research Council, Washington, DC, 1996, pp.65~71.
7. Bazant, Z. P. and Wu, S. T., "Creep and Shrinkage Law for Concrete at Variable Humidity", *Journal of Engineering Mechanics*, ASCE, Vol.100, No.6, 1974, pp.1183~1209.
8. Tang, T., Zollinger, D. G., and Senadheera, S. P., "Analysis of Concave Curling in Concrete Slabs", *Journal of Transportation Engineering*, ASCE, Vol.119, No.4, Jul.-Aug., 1993, pp. 618~633.
9. Ioannides, A. M. and Hammons, M. I., "Westergaard-Type Solution for Edge Load Transfer Problem", Transportation Research Record 1525, National Research Council, 1996, pp. 28~34.
10. Bazant, Z. P. and Najjar, L. J., "Nonlinear Water Diffusion in Nonsaturated Concrete", *Materials and Structures*, RILEM, Vol.5, No.25, 1972, pp.3~20.
11. ASTM, "*ASTM C 309: Standard Specification for Liquid Membrane-Forming Compounds for Curing Concrete*", Annual Book of ASTM Standards, American Society for Testing and Materials, West Conshohocken, PA, 1999.